Available online at www.sciencedirect.com
ScienceDirect
Journal of Hazardous Materials 154 (2008) 1025–1032
Journal of Hazardous Materials
www.elsevier.com/locate/jhazmat

Mechanism of *p*-nitrophenol adsorption from aqueous solution by HDTMA$^+$-pillared montmorillonite—Implications for water purification

Qin Zhou [a,b,c], Hong Ping He [a,c,*], Jian Xi Zhu [a], Wei Shen [a,b], Ray L. Frost [c,**], Peng Yuan [a]

[a] *Guangzhou Institute of Geochemistry, Chinese Academy of Sciences, Guangzhou 510640, China*
[b] *Graduate University of Chinese Academy of Sciences, Beijing 100039, China*
[c] *Inorganic Materials Research Program, School of Physical and Chemical Sciences, Queensland University of Technology, GPO Box 2434, Brisbane, Qld 4001, Australia*

Received 2 August 2007; received in revised form 27 September 2007; accepted 5 November 2007
Available online 13 November 2007

Abstract

HDTMA$^+$-pillared montmorillonites were obtained by pillaring different amounts of the surfactant hexadecyltrimethylammonium bromide (HDTMAB) into sodium montmorillonite (Na-Mt) in an aqueous solution. The optimum conditions and batch kinetics of sorption of *p*-nitrophenol from aqueous solutions are reported. The solution pH had a very important effect on the sorption of *p*-nitrophenol. The maximum *p*-nitrophenol absorption/adsorption occurs when solution pH (7.15–7.35) is approximately equal to the pK_a (7.16) of the *p*-nitrophenol ion deprotonation reaction. X-ray diffraction analysis showed that surfactant cations had been pillared into the interlayer and the *p*-nitrophenol affected the arrangement of surfactant. With the increased concentration of surfactant cations, the arrangement of HDTMA$^+$ within the clay interlayer changes and the sorption of *p*-nitrophenol increases. HDTMA$^+$-pillared montmorillonites are more effective than Na-Mt for the adsorption of *p*-nitrophenol from aqueous solutions. The Langmuir, Freundlich and dual-mode sorption were tested to fit the sorption isotherms.

Keywords: Adsorption; Depollution; Organoclay; Surfactant; Mechanism of adsorption

1. Introduction

As is well known, montmorillonite possesses a structure with two silica-oxygen tetrahedral sheets sandwiching an aluminium octahedral sheet, in which an aluminium ion is octahedrally coordinated to four oxygens and two hydroxyls. Due to the isomorphic substitution within the layers (for example, Al^{3+} replaced by Mg^{2+} or Fe^{2+} in the octahedral sheet; Si^{4+} replaced by Al^{3+} in the tetrahedral sheet), the clay layer is negatively charged, which is counterbalanced by the exchangeable cations (e.g. alkali-metal Na^+ and alkaline-earth-metal Ca^{2+}) in the interlayer. Because of the hydration of inorganic cations on the exchange sites, the clay mineral surface is hydrophilic in nature, which makes natural clays ineffective sorbents for organic compounds. Hence, the modification of the clay mineral surface with cationic surfactants, converts the normally hydrophilic silicate surface to an lipophilic surface, is a strategic step in the preparation of clay-based sorbents for organic pollutants [4].

Various organoclays have been synthesized using a range of surfactants, including single and dual cationic surfactants [29,33,38,45], anionic–cationic surfactants [27,42,43] and nonionic surfactants [28]. There are many applications about organoclays, for example, as adsorbents for the organic pollutants [25,31,42–45] and the air sampling of airborne organic contaminants [11], as components of earth landfill liners [30], as the transport of nonionic contaminants in ground water [32], as rheological control agents [24], as reinforcing fillers for plastics [34] and catalysts [6]. Different sorption mechanisms are demonstrated, strongly depending on the molecular structure of the organic pollutants and quaternary ammonium cations used to modify soil and clay. The small organic cations create a relatively rigid, nonpolar surface amenable to nonionic solute uptake by adsorption, whereas the large organic cations create an organic partition medium through the conglomeration of their

* Corresponding author at: Inorganic Materials Research Program, School of Physical and Chemical Sciences, Queensland University of Technology, GPO Box 2434, Brisbane, Qld 4001, Australia. Tel.: +86 20 85290257; fax: +86 20 85290130.
** Corresponding author. Tel.: +61 7 3138 2407; fax: +61 7 3138 1804.
E-mail addresses: hehp@gig.ac.cn (H.P. He), r.frost@qut.edu.au (R.L. Frost).

0304-3894/$ – see front matter © 2007 Elsevier B.V. All rights reserved.
doi:10.1016/j.jhazmat.2007.11.009

alkyl chains [5,29,30]. Thus these authors showed that sorption of NOCs (non-volatilization organic compounds) by large-alkyl organobentonites is essentially due to linear solute partitioning into the microscopic organic phase formed by the large alkyl chains of quaternary ammonium cation. Nonlinear isotherms indicative of adsorption or coadsorption were observed when small-alkyl organobentonites were used as sorbents [23,42]. The adsorption was characterized by nonlinear isotherms, strong solute uptake and competitive sorption, on the contrary, the partition was characterized by linear isotherms, relatively weak solute uptake and noncompetitive sorption [29].

As indicated by previous studies, characteristics of the surfactants used and organic pollutants have a significant influence on the adsorption capacity of organoclays. The adsorption capacity of organoclays increases with the surfactant loadings within the clay interlayer [13,15,21,40]. XRD analysis, combined with other techniques (e.g. FTIR, TG, MAS NMR and TEM), has demonstrated that the arrangement of surfactant in the clay interlayer space will vary from lateral-monolayer, to lateral-bilayer, then to paraffin-type monolayer and finally to paraffin-type bilayer with increased surfactant packing density [13,15,21,40]. However, both experimental and molecular modeling studies have shown that the structure of organoclay not only depends on the loading of the surfactant but also the charge density of the clay [14]. This means that the intercalated surfactants may take various arrangement models in different montmorillonites even if the surfactant loadings are the same. Wang et al. [33] found that the pore structure and surface characteristics of organoclays were closely related to the arrangement of surfactant in the interlayer. This means that the surfactant arrangement model might have a prominent effect on the adsorption capacity of organoclays. To the best of our knowledge, there are few studies which take into account the high surfactant packing density of organoclay and attempt to correlate the surfactant arrangement model and adsorption capacity of organoclay [7]. This is of great importance for the understanding of the adsorption mechanism and the selection of organoclays for wastewater treatment, remediation of contaminated soils and groundwater purification.

Hence, the main aim of this study is to establish relationships between the surfactant arrangement model and adsorption capacity of organoclays and demonstrate the sorption mechanism on the basis of adsorption model and spectroscopy. In this study, *p*-nitrophenol was chosen as the model pollutant because it is widely used in agriculture, dyes/pigments, engineering polymers and pharmaceuticals and as fungicide for leather, production of parathion and organic synthesis [26].

2. Experimental

2.1. Materials

Montmorillonite used is primarily a Ca-Mt from Neimeng, China. Its cation exchange capacity (CEC) is 90.8 mmol/100 g. The *p*-nitrophenol and hexadecyltrimethylammonium bromide (HDTMAB) used are of analytical grade and provided by YuanJu Chem. Co. Ltd., China. The aqueous solubility of *p*-nitrophenol is 1.6×10^4 mg/L at 25 °C.

2.2. Preparation of organoclays

The pure Ca-Mt was added to Na_2CO_3 solution, stirred for 3 h at 800 rpm and drops of HCl were added into the suspension to dissolve the CO_3^{2-}. Then the suspension was washed several times with deionized water until it was chloride free and dried at 108 °C. Such treated montmorillonite is designated as Na-Mt. There has been significant advancement in the preparation of organoclays [40,41]. The clarifying surfactant solution was obtained when selected amounts of HDTMAB were added to hot distilled water. Then specific amounts of Na-Mt were added into the above-mentioned solution and the mixtures were stirred slightly in a 80 °C water bath for 2 h. The water/Na-Mt mass ratio is 10. Then the suspension was subsequently washed with distilled water four times. The moist solid material was dried at 60 °C and ground with a mortar. The obtained surfactant modified montmorillonites were labeled as 0.5CEC-Mt, 0.7CEC-Mt, 1.5CEC-Mt, 2.5CEC-Mt, respectively. Here, the prefix number means the added surfactant in the preparation solution (proportion vs. CEC), and the corresponding weight (Q_a) can be calculated from the equation:

$$Q_a = Q_m \,\mathrm{CEC} \times 10^{-3} Q_s M$$

Q_m is the quantity of the used montmorillonite, CEC is the cation exchange capacity of the used montmorillonite, Q_s is the desired quantity of the added surfactant proportion vs. CEC, and M is the molecular weight of the surfactant. The loaded surfactant within the resulting organoclay was evaluated from high-resolution thermogravimetric analysis as shown in Table 1.

2.3. Procedures for sorption

A total of 0.2 g of montmorillonite was combined with 30 ml of different concentrations (100–8000 mg/L) of *p*-nitrophenol solution (the initial pH 5.0) in 50 mL Erlenmeyer flasks with glass caps. The flasks were shaken for 6 h at 25 °C at 150 rpm. After being centrifuged at 3500 rpm for 10 min, the *p*-nitrophenol concentration in the aqueous phase was determined by a UV-260 spectrophotometer at 317 nm, the detection limits being 0.05 mg/L. The *p*-nitrophenol uptake on the organoclays was calculated by the following equation: $Q = (C_0 - C_t)V/m$, Q is the *p*-nitrophenol uptake, C_0 is the initial concentration,

Table 1
Structural parameters and surfactant loadings of Na-Mt and the organoclays

Sample	d_{001} (nm)	S_{BET} (m^2/g)	V_P (cm^3/g)	SL (%)	SL (vs. CEC)
Na-Mt	1.24	55	0.11	–	–
0.5CEC-Mt	1.48	12	0.06	9.73	0.33
0.7CEC-Mt	1.78	10	0.06	16.73	0.61
1.5CEC-Mt	2.23	4	0.04	28.19	1.19
2.5CEC-Mt	3.84	1	0.01	44.17	2.4

The above data is cited from Ref. [30]. S_{BET}: specific surface area; V_P: pore volume determined by BJH method from N_2 desorption isotherm; SL: surfactant loading within the corresponding organoclay, evaluated from high-resolution thermogravimetric analysis; SL (vs. CEC): surfactant loading expressed in CEC of montmorillonite (100 g).

C_t is the equilibrium concentration, V is the volume of *p*-nitrophenol solution and m is the mass of sorbents. During the sorption procedures, the loss of the *p*-nitrophenol by both photochemical decomposition and volatilization were found to be negligible during adsorption [42]. The obtained surfactant modified montmorillonites with adsorbed *p*-nitrophenol were labeled as 0.5CEC-Mt-4000, 0.7CEC-Mt-4000, 1.5CEC-Mt-4000, 2.5CEC-Mt-4000, respectively and the 4000 was the concentration of *p*-nitrophenol.

2.4. Characterization methods

2.4.1. X-ray diffraction

X-ray diffraction (XRD) patterns were recorded using Cu Kα radiation ($n = 1.5418$ Å) on a Philips PANalytical X' Pert PRO diffractometer operating at 40 kV and 40 mA with 0.25° divergence slit, 0.5° anti-scatter slit, between 1.5° and 20° (2θ) at a step size of 0.0167°. For XRD at low angle section, it was between 1° and 5° (2θ) at a step size of 0.0167° with variable divergence slit and 0.125° anti-scatter slit.

2.4.2. BET

N_2 adsorption–desorption isotherms were measured at liquid nitrogen temperature with a Micromeritics ASAP 2010 gas sorption analyzer (Micromeritics, Norcross, GA, USA). Before measurement, the samples were pre-heated at 80 °C under N_2 for ca. 24 h. The specific surface area was calculated by using the BET equation and the total pore volumes were evaluated from nitrogen uptake at relative pressure of ca. 0.99. The Barrett–Joyner–Halenda (BJH) method was used to evaluate the average pore diameter (APD).

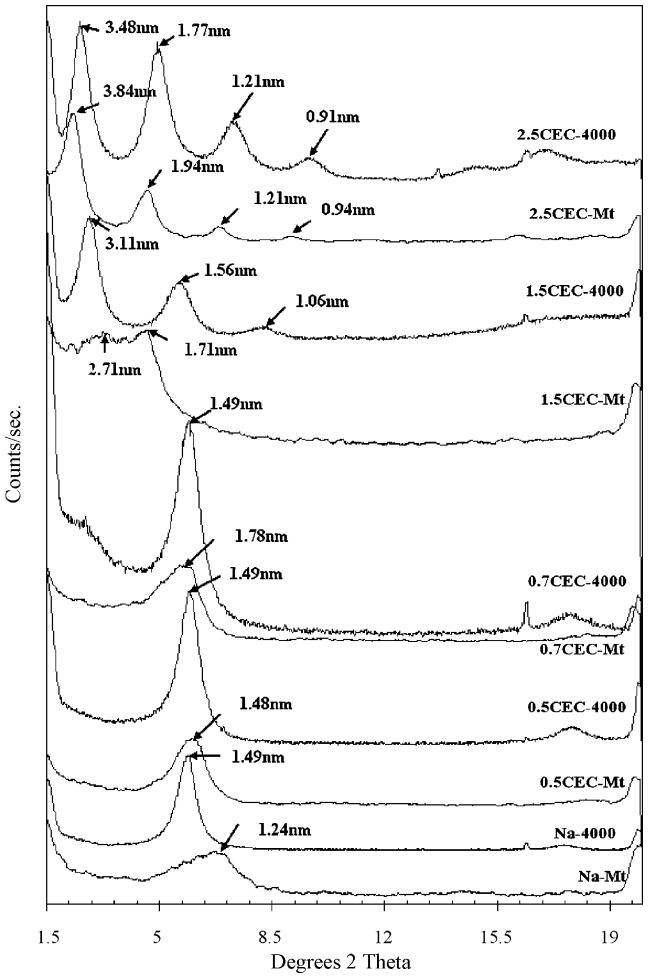

Fig. 1. XRD patterns of Na-Mt, organoclays and organoclays adsorbed *p*-nitrophenol.

3. Results and discussion

3.1. XRD

Expansion of the montmorillonites can be followed by measurement of the powder X-ray diffraction patterns. Fig. 1 shows the XRD patterns of Na-Mt, the organoclays and organoclays absorbed *p*-nitrophenol. With an increase of the loaded surfactant, the values of d_{001} increased gradually as follows: 1.24 nm (Na-Mt) → 1.48 nm (0.5CEC-Mt) → 1.78 nm (0.7CEC-Mt) → ca. 2.71 nm (broad peak, 1.5CEC-Mt) → 3.84 nm (2.5CEC-Mt). Thus the heights of the interlayer spacings of the corresponding organoclays were obtained by subtracting the thickness of TOT layer (0.96 nm) from the basal spacings, i.e., 0.52 nm (0.5CEC-Mt) → 0.82 nm (0.7CEC-Mt) → ca. 1.75 nm (1.5CEC-Mt) → 2.88 nm (2.5CEC-Mt) [TOT is the tetrahedral–octahedral–tetrahedral layer]. These results indicate that $HDTMA^+$ cations had been intercalated into the montmorillonite interlayer space. On the basis of the configuration of $HDTMA^+$ and the interlayer spacings of montmorillonite and the organoclays, different $HDTMA^+$ arrangement models within the montmorillonite interlayer space are proposed, i.e., lateral-monolayer in 0.5CEC-Mt, lateral-bilayer in 0.7CEC-Mt, paraffin-bilayer in 2.5CEC-Mt and a complex transition stage from lateral to paraffin arrangement in 1.5CEC-Mt as reported in literature [40,41].

The basal spacing for *p*-nitrophenol adsorbed on Na-Mt is 1.49 nm compared with 1.24 nm for the Na-Mt (Fig. 1). These numbers support the proposition that the *p*-nitrophenol has penetrated the clay interlayers and expanded the clay by an additional 0.25 nm which is close to the size of the *p*-nitrophenol molecule. The basal spacing for both the 0.5CEC-Mt and 0.5CEC-4000 is ~1.49 nm. However the basal spacings for 0.7CEC-4000 (1.49 nm) and 2.5CEC-4000 (3.48 nm) are less than that for 0.7CEC-Mt of 1.78 nm and 2.5CEC-Mt of 3.84 nm. This suggests that the *p*-nitrophenol has replaced some of the surfactant within the clay interlayers. The 3.11 nm basal spacing is ascribed to the surfactant and *p*-nitrophenol expanded montmorillonite for 1.5CEC-4000. The occurrence of the narrow peaks in 1.5CEC-4000, compared with that of 1.5CEC-Mt, indicates that the adsorbed *p*-nitrophenol has a significant effect on the arrangement of the intercalated organics. These values can be supported by our previous work [39] and suggest that the *p*-nitrophenol molecules are adsorbed in the interlayer of the Na-Mt and organoclays and effecting the arrangement of the surfactant molecules in the clay layers.

3.2. BET

The structure parameters of Na-Mt and the organoclays, including specific surface area (S_{BET}), total pore volume (V_P), and surfactant loading (SL) [17], are summarized in Table 1. Here, a dramatic decrease of the BET-N_2 surface area was observed from Na-Mt to 0.5CEC-Mt and 0.7CEC-Mt, then a pronounced decrease to 1.5CEC-Mt and 2.5CEC-Mt. A similar trend with a more smooth decrease was also found for the pore volumes of Na-Mt and the organoclays. Both S_{BET} and V_P decreases resulted from the increase of the loaded surfactant and their distribution [17].

3.3. Effect of pH

The solution pH value varied from 3 to 12 and the initial concentration of *p*-nitrophenol was 500 mg/L (pH_{in} 5.0). From Fig. 2, we can see that the *p*-nitrophenol removal on the organoclays increases with increasing the solution pH value when $pH < pK_a$ or $pH > 9$, but decreases with increasing the solution pH value when $9 > pH > pK_a$. *p*-Nitrophenol may exist as anion when the solution $pH > pK_a$ [44] and as molecule when the solution $pH < pK_a$. So the sorption result was affected by the competitive influence of increasing *p*-nitrophenol ion and *p*-nitrophenol ion-molecule complex formation. There are two main mechanisms for the sorption of *p*-nitrophenol on the Na-Mt and organoclays. One is electrostatic attraction when the *p*-nitrophenol exists as anion; the other is partition when the *p*-nitrophenol exists as molecule. But the *p*-nitrophenol removal keeps on increasing when the $pH > 9$, this result can be explained by Eq. (1) [3], which expresses the degree of *p*-nitrophenol ionization increases when the pH value increases. φ_{ions} is the degree of *p*-nitrophenol ionization (the result is showed in Table 2). Considering the practical application, we can think that the maximum *p*-nitrophenol adsorption occurs when solution pH is approximately equal to the pK_a of the *p*-nitrophenol ion deprotonation reaction. Many previous published reports on the effect of pH on the adsorption of *p*-nitrophenol have shown variations in the experimental results because of the different experimental conditions used in their experiments [9,20]:

$$\varphi_{ions} = \frac{1}{1 + 10^{(pK_a - pH)}} \quad (1)$$

Table 2
The extent of *p*-nitrophenol ionization at different pH values

pH	φ_{ions}
3	6.92×10^{-5}
4	6.91×10^{-4}
5	6.87×10^{-3}
6	0.065
7	0.41
8	0.87
9	0.98
10	0.999
11	1
12	1

3.4. Sorption kinetics

The relationship between reaction time and sorption amounts of *p*-nitrophenol was presented in Fig. 3. Such plots may indicate that two or more adsorption steps occur. The first portion is fast characterized by rapid attachment of *p*-nitrophenol to the surface or the interlayer of the sorbent. The second portion is slower due to the repulsive force. The third is the equilibrium stage. The process is similar to the adsorption of phenol using activated bentonites reported by Al-Ashen et al. [2]. The equilibrium time required for the adsorption of *p*-nitrophenol was almost 20 min; however, to ensure equilibrium, the subsequent experiments were left for 6 h.

Several simplified kinetic models including the pseudo-first-order equation, pseudo-second-order equation, and intraparticle diffusion model were used to test the experimental data to examine the mechanism of adsorption processes.

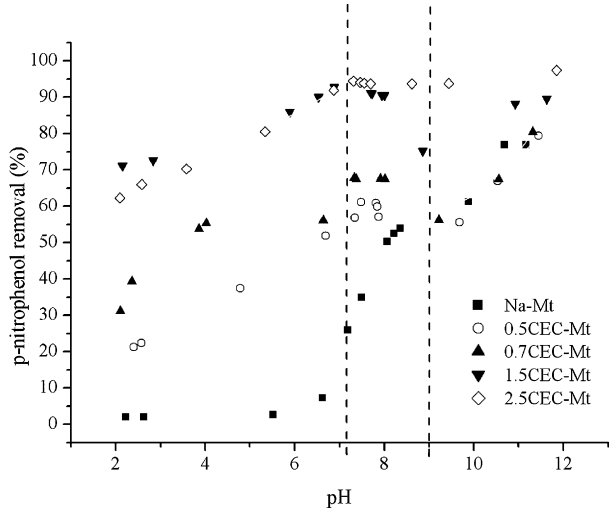

Fig. 2. The relationship between pH_{eq} values and *p*-nitrophenol removal (25 °C, 500 mg/L).

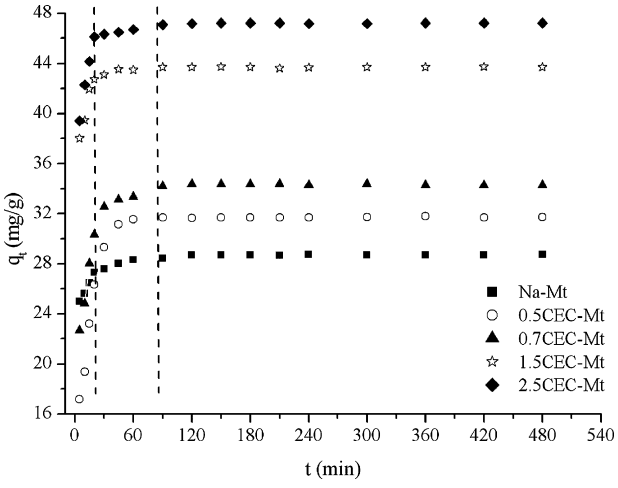

Fig. 3. The relationship between *p*-nitrophenol uptake and reaction time (25 °C, 500 mg/L).

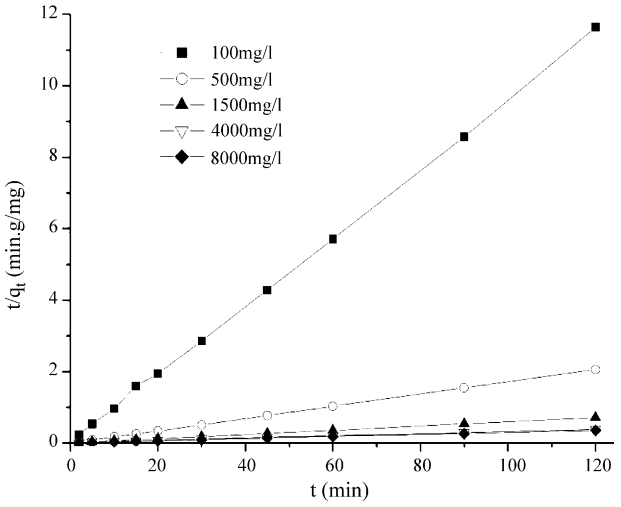

Fig. 4. Test of the pseudo-second-order equation for the sorption of *p*-nitrophenol (25 °C, 1.5CEC-Mt).

A simple kinetic analysis of adsorption was the Lagergren rate equation [22], which was the first rate equation for the sorption of liquid/solid system based on solid capacity and one of the most widely used sorption rate equations for the sorption of a solute from a liquid solution. It may be expressed as

$$\frac{dq_t}{d_t} = k_1(q_{e1} - q_t), \tag{2}$$

where k_1 is the equilibrium rate constant of pseudo-first-order adsorption (min^{-1}), q_{e1} is the amount of adsorption at equilibrium (mg/g) and q_t is the amount of adsorption at time t (mg/g). After definite integration by applying the initial conditions $q_t = 0$ at $t = 0$ and $q_t = q_t$ at $t = t$, Eq. (2) becomes:

$$\ln(q_{e1} - q_t) = \ln q_{e1} - k_1 t. \tag{3}$$

But Aharoni and Sparks [1] thought the equation applicable to experimental results generally differed from a true order equation two ways, thus Eq. (4) was formed on the basis of Eq. (3):

$$\ln(q_e - q_t) = \ln q_e - k(t + t_0), \tag{4}$$

where t_0 is an adjustable parameter that makes q_e suitable for the use in the kinetic expression.

On the other hand, a pseudo-second-order equation based on adsorption capacity may be represented in the following:

$$\frac{dq_t}{d_t} = k_2(q_{e2} - q_t)^2, \tag{5}$$

where k_2 is the rate constant of pseudo-second-order adsorption. Applying the initial conditions, the integrated form of Eq. (5) becomes

$$\frac{t}{q_t} = \frac{1}{(k_2 q_{e2}^2)} + \frac{t}{q_{e2}} \tag{6}$$

The parameters k_2 and q_{e2} are obtained from the linear plot of t/q_t vs. t, as shown in Fig. 4. The pseudo-first-order model cannot fit the experiment and all the other constants are presented in Table 3.

In fact pseudo-second-order kinetic model has a better relativity than the modified pseudo-first-order model.

Another intraparticle diffusion model proposed by Weber and Morris [35] was applied because the above models cannot identify the diffusion mechanism. The fractional approach to equilibrium changes according to a function of $(Dt/r2)^{1/2}$, where r is the particle radius and D is the diffusivity of solutes within the particle. The initial rate of intraparticle diffusion can be obtained by linearization of the curve $q_t = f(t^{1/2})$ [19]. Weber and Morris [35] reported that if intraparticle diffusion was involved in the sorption process, then a plot of the square root of time vs. the adsorption amount would result in a linear relationship, and that the particle diffusion would be the controlling step if this line passes through the origin. Fig. 5 shows that every line is similar to be straight one but none passes through the origin. So it indicates that particle diffusion is involved in the sorption process, but it is not the controlling step. Simultaneously, because the pseudo-second-order model is basically based on the sorption capacity, the description of sorption suggests that the chemical reaction is rate controlling [20].

3.5. Sorption mechanism

Several sorption models [20] such as Langmuir model (LM), Freundlich model (FM) and dual-mode sorption model (DSM) [10] were used to examine the experimental data and the equations were followings:

$$q = \frac{q_L K_L C_e}{1 + K_L C_e} \quad \text{(LM)},$$

Table 3
Model parameters for sorption of the *p*-nitrophenol onto the 1.5CEC-Mt at 25 °C

Initial concentration (mg/g)	The modified pseudo-first-order				Pseudo-second-order		
	k (min^{-1})	q_e (mg/g)	t_0 (min)	R^2	k_2 (min^{-1})	q_{e2} (mg/g)	R^2
100	0.13806	10.42509	10.8252	0.80698	0.30	10.44	0.9996
500	0.29011	58.53033	9.53757	0.90201	0.15	58.38	1.0
1500	0.08155	168.62457	29.13707	0.91413	0.0181	169.20	1.0
4000	0.02556	313.03681	48.34083	0.95392	0.001	314.47	0.998
8000	0.062	325.80014	72.1564	0.83689	0.0032	341.30	0.9995

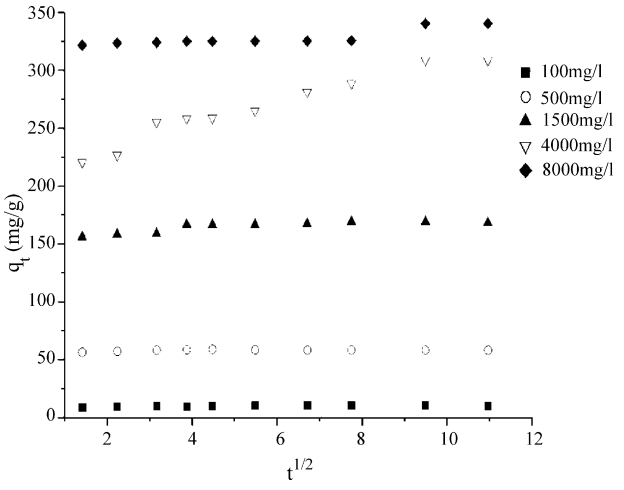

Fig. 5. The relationship between *p*-nitrophenol uptake and square root of reaction time with different initial concentrations of *p*-nitrophenol (25 °C, 1.5CEC-Mt).

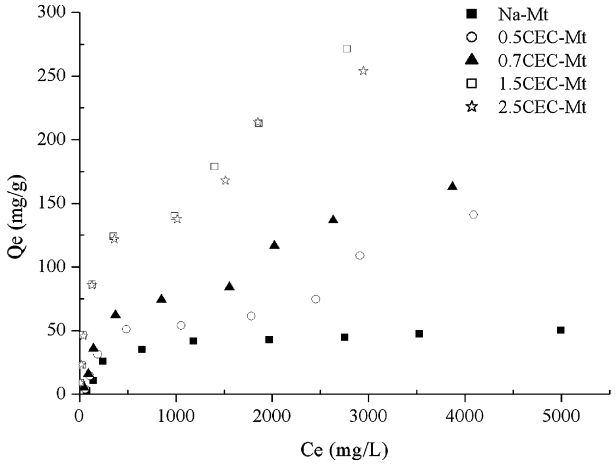

Fig. 6. Adsorption isotherms of *p*-nitrophenol in the Na-Mt and $HDTMA^+$-pillared montmorillonites (25 °C).

$$q = K_F C_e \frac{1}{n} \quad \text{(FM)},$$

$$q = K_H C_e + \frac{q_{DS} K_{DS} C_e}{1 + K_{DS} C_e} \quad \text{(DSM)},$$

where C_e is the equilibrium concentration of *p*-nitrophenol, q is the sorbed amount to per unit mass of clay, q_L, q_{DS}, and K_L, K_{DS} denote monolayer sorption capacity and sorption constant, respectively. All the parameters in the above-mentioned models based on the experiments are determined using the optimization procedure based on least-square algorithm and shown in Table 4.

Fig. 6 shows that the adsorbed amounts of *p*-nitrophenol onto Na-Mt and the organoclays and the adsorbing efficiency of the materials increases as Na-Mt < 0.5CEC-Mt < 0.7CEC-Mt < 1.5CEC-Mt ≈ 2.5CEC-Mt. Here, it can be seen that the adsorbed amounts of *p*-nitrophenol strongly depend on the loaded surfactant and their distributions.

As is well known, due to the isomorphic substitution within the layers, the montmorillonite layer is negatively charged, which is counterbalanced by the exchangeable cations in the interlayer [12]. In the case of Na-Mt which BET-N_2 surface area is largest, electrostatic attraction between the *p*-nitrophenol anions and hydrated metal cations is the main force for *p*-nitrophenol penetrating into montmorillonite interlayer space and resulting in the expansion of the clay interlayer as shown by XRD pattern.

Previous studies [17,20] have demonstrated that the surfactant cations/molecules not only enter into the clay interlayer space but also are sorbed outside the clay interlayer. When the surfactant concentration is relatively low (e.g. 0.5CEC-Mt and 0.7CEC-Mt), the surfactant cations prefer to enter into the montmorillonite interlayer space by replacing the interlayer exchangeable cations [16,17,36,37]. With the increase of the $HDTMA^+$ cations, the large intercalated $HDTMA^+$ cations may result in serious blocking of the interlamellar space that inhibits the passage of nitrogen molecules, leading to a decrease of BET-N_2 surface area and pore volume of the organoclays. Our recent study [17] and other literatures [20] show that, when the surfactant loading more than the montmorillonte's CEC (1.5CEC-Mt and 2.5CEC-Mt), there are three different distribution/location types of surfactant, including the surfactant cations and ion pairs ($HDTMA^+$ and Br^-) located in the interlayer spaces, and surfactant occupying the pores available between clay particles with a "house of cards" structure. Obviously, two basic organoclay types are formed when modifying clay with surfactant on the basis of the distribution of surfactant: (1) the surfactant mainly occupies the clay interlayer space and (2) both the clay interlayer space and external surface are modified by surfactant. This conclusion is strongly supported by our recent studies on the corresponding organoclays using BET-N_2, high-resolution thermogravimetry (HRTG) and XPS [16,17].

The surfactant located within the interlayer spaces and interparticle pores can form micelles, which play an important role to adsorb the organic pollutants [18] when the concentra-

Table 4
Model parameters for the sorption of *p*-nitrophenol on Na-Mt and organoclays at 25 °C

	Langmuir model [38]			Freundlich model (FM)			Dual-mode sorption model (DSM)			
	K_L (l/mg)	q_L (mg/g)	R^2	K_F (l/g)	$1/n$	R^2	K_H (l/g)	K_{DS} (l/mg)	q_{DS} (mg/g)	R^2
Na-Mt	0.00081	83.49256	0.97599	2.66782	0.36897	0.88844	0	0.00081	83.49518	0.97599
0.5CEC-Mt	0.00078	174.34004	0.98752	4.54181	0.39292	0.92187	0.0003	0.00081	170.96113	0.98755
0.7CEC-Mt	0.0014	184.31147	0.96603	9.14691	0.33006	0.85498	0.00099	0.00129	193.3343	0.96657
1.5CEC-Mt	0.0016	375.54674	0.98104	19.3044	0.33025	0.88641	0.00481	0.00133	416.8485	0.98103
2.5CEC-Mt	0.0019	435.7856	0.96536	26.80378	0.31166	0.8428	0.01276	0.00132	539.6637	0.9747

tion is higher than the critical micelle concentration (CMC). For 0.5CEC-Mt and 0.7CEC-Mt, the surfactant cations in the interlayer space have two influences on the adsorption of *p*-nitrophenol onto the organoclays. The electrostatic attraction between the *p*-nitrophenol anions and surfactant cations leads *p*-nitrophenol anions entering into the interlayer. Meanwhile, the organic micelles formed by the intercalated surfactant are an excellent medium for partition of *p*-nitrophenol. In the case of 1.5CEC-Mt and 2.5CEC-Mt, the clay layers are almost completely enclosed by surfactant and an organic medium can be visualized as formed within the clay layer space and in the interparticle pores. This organic medium is of high importance for the excellent affinity between organoclay and organic pollutants, and is available as a partition medium for contaminant sorption [5,8]. Accordingly, the sorption efficiency of the corresponding organoclays is obviously higher than that of Na-Mt. This suggests that the distribution and arrangement of surfactant in the organoclays control sorption efficiency and mechanism rather than BET-N_2 surface area, pore volume and pore diameter [17].

Meanwhile, the DSM model has a better fit than others and the result also assumes the sorption mechanism that some of solutes dissolve in the medium (partition) and the rest are adsorbed onto the sorption sites (adsorption) on the organoclays. Adsorption is the main reaction for the 0.5CEC-Mt and 0.7CEC-Mt and partition is the main one for the 1.5CEC-Mt and 2.5 CEC-Mt.

4. Conclusions

With the increase of the concentration of $HDTMA^+$ cations, the arrangement of $HDTMA^+$ changes and the sorption amounts of *p*-nitrophenol increase. $HDTMA^+$ pillared montmorillonites are more effective than Na-Mt for the adsorption of *p*-nitrophenol from aqueous solutions. The resulting concentration of *p*-nitrophenol can reach the effluent standard for low concentration waste water (<100 mg/L) and is close to the effluent standard for middle concentration waste water (<500 mg/L). The sorption process of *p*-nitrophenol from aqueous solutions includes partition and adsorption basis of the sorbents.

Acknowledgements

This work was supported by the grant of the Knowledge Innovation Program of the Chinese Academy of Sciences (Grant No. Kzcx2-yw-112) and Natural Science Foundation of Guangdong Province (Grant No. 05103410). The Inorganic Materials Research Program, Queensland University of Technology, is gratefully acknowledged for infra-structural support.

References

[1] C. Aharoni, D.L. Sparks, S. Levinson, I. Ravina, Kinetics of soil chemical reactions: relationships between empirical equations and diffusion models. Soil Sci. Soc. Am. J. (1991) 55(5) 1307–1312. CODEN: SSSJD4 ISSN:0361-5995. CAN 116:5762 AN 1992:5762 CAPLUS.

[2] S. Al-Asheh, F. Banat, L. Abu-Aitah, Adsorption of phenol using different types of activated bentonites, Sep Purif. Technol. 33 (2003) 1–10.

[3] F.A. Banat, B. Al-Bashir, S. Al-Asheh, O. Hayajneh, Adsorption of phenol by bentonite, Environ. Pollut. 107 (2000) 391–398.

[4] F. Bergaya, G. Lagaly, Surface modification of clay minerals, Appl. Clay Sci. 19 (2001) 1–6.

[5] S.A. Boyd, J.F. Lee, M.M. Mortland, Attenuating organic contaminant mobility by soil modification, Nature 333 (1988) 345–349.

[6] C. Breen, R. Watson, J. Madejova, P. Komadel, Z. Klapyta, Langmuir 13 (1997) 6473–6479.

[7] B.L. Chen, L.Z. Zhu, J.X. Zhu, Configurations of the bentonite-sorbed myristylpyridinium cation and their influences on the uptake of organic compounds, Environ. Sci. Technol. 39 (2005) 6093–6100.

[8] Y. Chun, G.Y. Sheng, S.A. Boyd, Sorptive characteristics of tetraalkylammonium-exchanged smectite clays, Clay Clay Miner. 51 (2003) 415–420.

[9] K. Dong-Geun, S. Dong-Ik, J. Young-Woong, pH-dependent sorptions of phenolic compounds onto montmorillonite modified with hexadecyltrimethylammonium cation, Sep. Sci. Technol. 36 (2001) 3159–3174.

[10] A.H. Gemeay, A.S. El-Sherbiny, A.B. Zaki, Adsorption and kinetic studies of the intercalation of some organic compounds onto Na-Montmorillonite, J. Colloid Interf. Sci. 245 (2001) 116–125.

[11] P. Harper, Alkylammonium montmorillonites as adsorbents for organic vapors from air, Environ. Sci. Technol. 24 (1990) 1155–1161.

[12] H.P. He, Interaction of Clay Minerals and Heavy Metals, Petroleum Industry Publishing House, Beijing, 2001.

[13] H.P. He, Z. Ding, J.X. Zhu, P. Yuan, Y.F. Xi, D. Yang, R.L. Frost, Thermal characterization of surfactant-modified montmorillonites, Clay Clay Miner. 53 (2005) 287–293.

[14] H.P. He, R.L. Frost, T. Bostrom, P. Yuan, L.V. Duong, D. Yang, Y.F. Xi, T.J. Kloprogge, Changes in the morphology of organoclays with HDTMA(+) surfactant loading, Appl. Clay Sci. 31 (2006) 262–271.

[15] H.P. He, R.L. Frost, Y.F. Xi, J.X. Zhu, Raman spectroscopic study of organo-montmorillonites, J. Raman Spectrosc. 35 (2004) 316–323.

[16] H.P. He, Q. Zhou, R.L. Frost, B.J. Wood, L.V. Duong, T.J. Kloprogge, A X-ray photoelectron spectroscopy study of HDTMAB distribution within organoclays, Spectrochim. Acta A: Mol. Biomol. Spectrosc. 66 (2007) 1180–1188.

[17] H.P. He, Q. Zhou, N.M. Wayde, T.J. Kloprogge, P. Yuan, Y.F. Xi, J.X. Zhu, R.L. Frost, Microstructure of HDTMA+-modified montmorillonite and its influence on sorption characteristics, Clay Clay Miner. 54 (2006) 691–698.

[18] P. Jae-Woo, R.J. Peter, Partitioning of three nonionic organic compounds between adsorbed surfactants, micelles, and water, Environ. Sci. Technol. 27 (1993) 2559–2565.

[19] M. Jansson-Charrier, E. Guibal, J. Roussy, B. Delanghe, C.P. Le, Vanadium (IV) sorption by chitosan: kinetics and equilibrium, Water Res. 30 (1996) 465–475.

[20] R.S. Juang, S.H. Lin, K.H. Tsao, Mechanism of sorption of phenols from aqueous solutions onto surfactant-modified montmorillonite, J. Colloid Interf. Sci. 254 (2002) 234–241.

[21] G. Lagaly, Characterization of clays by organic compounds, Clay Miner. 16 (1981) 1–21.

[22] S. Lagergren, About the theory of so-called adsoption of solute substances. Handlingar, 1898.

[23] J.F. Lee, M.M. Mortland, C.T. Chiou, D.E. Kile, S.A. Boyd, Adsorption of benzene, toluene, and xylene by tetramethylammonium-smectites having different charge densities, Clays Clay Miner. 38 (1990) 113–120.

[24] E. Manias, G. Hadziioannou, G. Brinke, Inhomogeneities in sheared ultrathin lubricating films, Langmuir 12 (1996) 4587–4593.

[25] L.P. Meier, R. Nueesch, F.T. Madsen, Organic pillared clays, J. Colloid Interf. Sci. 238 (2001) 24–32.

[26] J.H. Montgomery, L.M. Welkom, Groundwater Chemicals Desk Reference, Lewis Publishers, Inc., Chelsea, MI, 1990.

[27] O. Regev, A. Khan, Alkyl chain symmetry effects in mixed cationic–anionic surfactant systems, J. Colloid Interf. Sci. 182 (1996) 95–109.

[28] Y.H. Shen, Preparations of organobentonite using nonionic surfactants, Chemosphere 44 (2001) 989–995.

[29] J.A. Smith, A. Galan, Soption of nonionic organic contaminants to single and dual organic cation bentonites from water, Environ. Sci. Technol. 29 (1995) 685–692.

[30] J.A. Smith, P.R. Jaffe, Benzene transport through landfill liners containing organophilic bentonite, J. Environ. Eng. 120 (1994) 1559–1577.

[31] M.R. Stackmeyer, Adsorption of organic compounds on organophilic bentonites, Appl. Clay Sci. 6 (1991) 39–57.

[32] J. Wagner, H. Chen, B.J. Brownawell, J.C. Westall, Use of cationic surfactants to modify soil surfaces to promote sorption and retard migration of hydrophobic organic compounds, Environ. Sci. Technol. 28 (1994) 231–237.
[33] C.C. Wang, L.C. Juang, C.K. Lee, T.C. Hsu, J.F. Lee, H.P. Chao, Effects of exchanged surfactant cations on the pore structure and adsorption characteristics of montmotrillonite, J. Colloid Interf. Sci. 280 (2004) 27–35.
[34] Z. Wang, T.J. Pinnavaia, Nanolayer reinforcement of elastomeric polyurethane, Chem. Mater. 10 (1998) 3769–3771.
[35] W.J. Weber, J.C. Morris, Kinetics of adsorption on carbon from solution, J. Sanitary Eng. Div. ASCE 89 (1963) 31–59.
[36] S.H. Xu, S.A. Boyd, Cationic surfactant adsorption by swelling and non-swelling layer silicates, Langmuir 11 (1995) 2508–2514.
[37] S.H. Xu, S.A. Boyd, Cationic surfactant sorption to a vermiculitic subsoil via hydrophobic bonding, Environ. Sci. Technol. 29 (1995) 312–320.
[38] N. Yilmaz, S. Yapar, Adsorption properties of tetradecyl- and hexadecyltrimethylammonium bentonites, Appl. Clay Sci. 27 (2004) 223–228.
[39] Q. Zhou, R.L. Frost, H.P. He, Y.F. Xi, Changes in the surfaces of adsorbed paranitrophenol on HDTMA organoclay—an XRD and TG study, J. Colloid Interf. Sci. 307 (2007) 50–55.
[40] J.X. Zhu, H.P. He, J.G. Guo, D. Yang, X.D. Xie, Arrangement models of alkylammonium cations in the interlayer of HDTMA+ pillared montmorillonites, Chin. Sci. Bull. 48 (2003) 368–372.
[41] J.X. Zhu, H.P. He, J.G. Guo, D. Yang, X.D. Xie, Study on the relationship between the arrangement models of organic cation in HDTMA+-montmorillonite and its theoretic sizes, J. Mineral. Petrol. 23 (2003) 1–4.
[42] L.Z. Zhu, B.L. Chen, Sorption behavior of *p*-nitrophenol on the interface between anion–cation organobentonite and water, Environ. Sci. Technol. 34 (2000) 2997–3002.
[43] L.Z. Zhu, B.L. Chen, X.Y. Shen, Sorption of phenol, *p*-nitrophenol and aniline to dual-cation organobentonites from water, Environ. Sci. Technol. 34 (2000) 468–475.
[44] L.Z. Zhu, J.Z. Hu, X.Q. Shen, J. Chai, Organobentonites as adsorbents for *p*-nitrophenol and its application in water treatment, J. Environ. Sci. 15 (1995) 316–321.
[45] L.Z. Zhu, X.G. Ren, S.B. Yu, Use of cetyltrimethylammonium bromide bentonite to remove organic contaminants of varying polar character from water, Environ. Sci. Technol. 32 (1998) 3374–3378.